ACS APPLIED MATERIALS & INTERFACES

Research Article

www.acsami.org

High Through-Plane Thermal Conduction of Graphene Nanoflake Filled Polymer Composites Melt-Processed in an L-Shape Kinked Tube

Haejong Jung,[†,∥] Seunggun Yu,[†,∥] Nam-Seok Bae,[†] Suk Man Cho,[†] Richard Hahnkee Kim,[†] Sung Hwan Cho,[†] Ihn Hwang,[†] Beomjin Jeong,[†] Ji Su Ryu,[‡] Junyeon Hwang,[‡] Soon Man Hong,[§] Chong Min Koo,*[,§] and Cheolmin Park*[,†]

[†]Department of Materials Science and Engineering, Yonsei University, Seoul, 120-749, Republic of Korea

[‡]Carbon Convergence Materials Research Center, Korea Institute of Science and Technology, Jeonbuk 565-905, Republic of Korea

[§]Materials Architecturing Research Center, Korea Institute of Science and Technology, Seoul, 136-791, Republic of Korea

Supporting Information

ABSTRACT: Design of materials to be heat-conductive in a preferred direction is a crucial issue for efficient heat dissipation in systems using stacked devices. Here, we demonstrate a facile route to fabricate polymer composites with directional thermal conduction. Our method is based on control of the orientation of fillers with anisotropic heat conduction. Melt-compression of solution-cast poly(vinylidene fluoride) (PVDF) and graphene nanoflake (GNF) films in an L-shape kinked tube yielded a lightweight polymer composite with the surface normal of GNF preferentially aligned perpendicular to the melt-flow direction, giving rise to a directional thermal conductivity of approximately 10 W/mK at 25 vol % with an anisotropic thermal conduction ratio greater than six. The high directional thermal conduction was attributed to the two-dimensional planar shape of GNFs readily adaptable to the molten polymer flow, compared with highly entangled carbon nanotubes and three-dimensional graphite fillers. Furthermore, our composite with its density of approximately 1.5 g/cm^3 was mechanically stable, and its thermal performance was successfully preserved above 100 °C even after multiple heating and cooling cycles. The results indicate that the methodology using an L-shape kinked tube is a new way to achieve polymer composites with highly anisotropic thermal conduction.

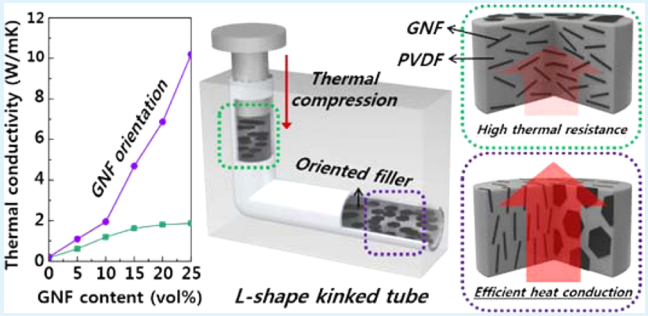

KEYWORDS: *thermal conductivity, graphene nanoflake, L-shape kinked tube, orientation, polymer composite, poly(vinylidene fluoride)*

INTRODUCTION

Management of undesired heat accumulated in high-performance photoelectronic components and systems, such as light emitting diodes, CMOS, and power generation and storage systems, is extremely important for reliable device operation.[1−6] Efficient heat release from these devices requires thermally conductive materials between heat sources and heat sinks. In particular, thermal conduction materials based on polymer filled systems have attracted great attention because of their low-temperature processing, resulting in cost-effectiveness, low density, and easy shape-forming capability suitable for integrated microdevices with complicated topographic geometries.[7,8] Considering that conventional high thermal conduction composites with thermally conductive particles require a high volume fraction (>50 vol %) of the fillers to obtain through-plane thermal conductivity (K) values of approximately 1−5 W/mK at room temperature, there is need for a polymer composite with high K but low filler loading and composite density.[9−11]

Although numerous works have attempted to elucidate the thermal conduction mechanism of such a filled system based on percolation theory at a very low filler loading condition,[12,13] a universal conclusion has not yet been derived because of the difficulty in understanding a composite with many different thermally resistive interfaces and contacts.[14,15] These thermal boundary resistances (TBRs) have made it even more difficult to develop high-K composites for practical applications. Efficient control of the TBR is essential for designing high-performance K polymer composites. Therefore, a robust route for significantly reducing TBR is in high demand.[16,17] One promising approach to control TBRs is to align fillers with anisotropic shape along the through-plane heat conductive direction. For instance, nanoscale fillers such as carbon nanotubes and boron nitride aligned by external fields, as

Received: April 2, 2015
Accepted: June 29, 2015
Published: June 29, 2015

DOI: 10.1021/acsami.5b02681
ACS Appl. Mater. Interfaces 2015, 7, 15256−15262

well as directional growth of the tubes, efficiently produce heat conduction pathways, thereby leading to enhanced K of the composite[18−23] (Supporting Information Table S1). Previous studies were, however, hardly successful to achieve the performance required for real applications, mainly because of insufficient alignment of the fillers with limited direct contact.

In this work, we demonstrate high-performance polymer composites with two-dimensional graphene nanoflakes (GNFs) dispersed and directionally aligned in a polymer matrix. Our method is based on the orientation of GNFs in thermoplastic poly(vinylidene fluoride) (PVDF) melt-compressed through a 90° L-shape kinked tube, as shown in Figure 1. Laminar flow of

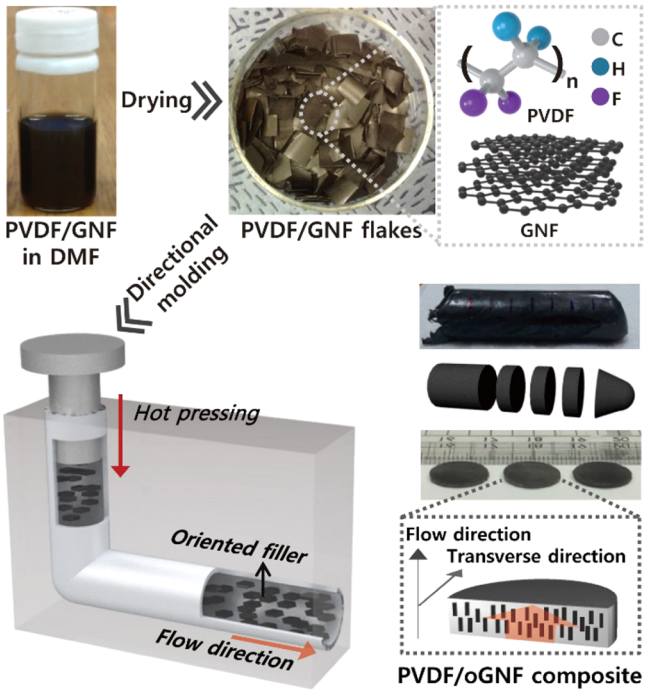

Figure 1. Schematic illustration of the fabrication process of GNFs preferentially aligned in PVDF through an L-shaped kinked tube. Photographs in the right bottom side show a cylindrical oGNF/PVDF composite and the disk-type specimens for thermal conductivity measurement sliced and polished from the cylindrical composite. Proposed orientation of GNFs developed during the process is also shown in the schematic.

the molten composite without turbulence was triggered by vertical compression of stacked GNFs, whose surface was oriented perpendicular to the flow direction (FD). At an optimized composite composition (25 vol % of GNFs), our lightweight composite with a density of 1.5 g/cm^3 exhibited a through-plane K of approximately 10 W/mK. Systematic investigation with other carbon-based fillers such as nanotubes and graphite revealed that the two-dimensional planar shape of GNFs was readily adaptable to flow field and was responsible for the highly directional thermal conduction with an anisotropic conduction ratio greater than six. Furthermore, our composite was heat-resistive even above 100 °C and was durable after multiple heating and cooling cycles.

EXPERIMENTAL SECTION

Materials. PVDF with a molecular weight of 275 000 g/mol and *N*,*N*′-dimethylformamide (DMF) were purchased from Sigma-Aldrich. Multiwalled carbon nanotubes (MWCNTs) with a diameter of 10−15 nm and a length of 100 μm were purchased from Hanwha Nanotech. GNFs with a diameter of 5 μm and a thickness of 6−8 nm were purchased from XG Sciences. Graphite with a diameter of 45 μm and a thickness of 3−5 μm was purchased from Shuangxing Industrial Co., Ltd., China.

Preparation of PVDF/GNF Composites. An appropriate amount of PVDF was dissolved in DMF for 6 h at 120 °C. The PVDF solution was mixed with various carbon fillers via bath sonication for 2 h to homogeneously disperse the fillers. The PVDF/GNF composites were obtained by evaporating the DMF solvent for 12 h at 140 °C. The as-prepared PVDF/GNF was then cut, resulting in pieces of thin mat suitable for packing into a mold.

Preparation of PVDF/oGNF Composites. To induce GNF orientation, we used a custom-made mold package. The mold consisted of an inner tube with a 90° kinked L-shape and bottom and side cylinder pistons (Supporting Information Figure S1). The pieces of PVDF/GNF composite mat were placed into the top entrance of the mold with a diameter of 1.27 cm and then hot-pressed at a pressure of 10 MPa at 180 °C for 5 min. After releasing the side piston, the mixture was further compressed, leading to orientation of GNF in the composite by filling the kinked parallel tube. The PVDF with oriented GNF in a pillar shape was carefully polished to a thickness of 0.2 cm for thermal conductivity measurement. A sample prepared at a pressure lower than 10 MPa was broken down during the polishing process, making it rarely possible to measure the thermal conduction properties of the sample. At high pressure greater than 10 MPa, on the other hand, a composite was hardly obtained mainly due to the overflow of molten composite arising from the leakage through a compressing cylinder gap. For comparison, the controlled PVDF/GNF composites were fabricated by direct thermal compression of the composite mat at a pressure of 10 MPa at 180 °C for 5 min without using the 90 deg-kinked L-shape mold.

Characterization. Thermal diffusivity of the composites was measured using the laser flash method (LFA-447, Netzsch, Germany) based on a xenon flash lamp source. The specific heat was determined from this technique and then compared with that of a pyroceramic reference sample. The thermal conductivity was determined from the equation $K = T_d \times \rho \times C_p$, where T_d, ρ, and C_p are the thermal diffusivity (cm^2/s), density (g/cm^3), and specific heat capacity (J/kg K), respectively. For the heating and cooling cycle test, the composites were heated to 100 °C at 5 °C/min and allowed to cool naturally to room temperature. Thermal expansion behavior was evaluated using thermomechanical analysis (TMA-Q400, TA Instruments) between 30 and 150 °C at 10 °C/min. The morphologies of MWCNT, GNF, graphite, controlled PVDF/GNF, and PVDF/oriented GNF (oGNF) composites were analyzed using a field emission scanning electron microscope (FEI Inspect F50). The orientation feature of fillers in the composites was evaluated by X-ray diffraction with a micro-diffractometer (Bruker-AXS) and CuKα radiation (40 kV and 40 mA) using a 2D detector. The distance between the sample and detector was 3 cm. Thermal imaging analysis was performed using a conventional infrared camera (T360, FLIR). Thermal properties of PVDF were examined with differential scanning calorimetry (Q-20, TA Instruments). Electrical conductivity was examined with sheet resistance using a four-point-probe measurement system (CRESBOX, Napson, Japan).

RESULTS AND DISCUSSION

Figure 1 schematically illustrates the fabrication process of GNFs oriented and embedded in PVDF by melt compression through an L-shape kinked tube. We choose a thermoplastic PVDF matrix because of its excellent thermo-mechanical properties.[24] In addition, PVDF has been widely investigated in a composite with CNTs for high K and electrically conductive composite applications.[25−27] First, to achieve homogeneous GNF dispersion in the PVDF matrix, a mixture of PVDF and GNFs was prepared in DMF, followed by evaporation of the solvent. In this step of Figure 1, an

DOI: 10.1021/acsami.5b02681
ACS Appl. Mater. Interfaces 2015, 7, 15256−15262

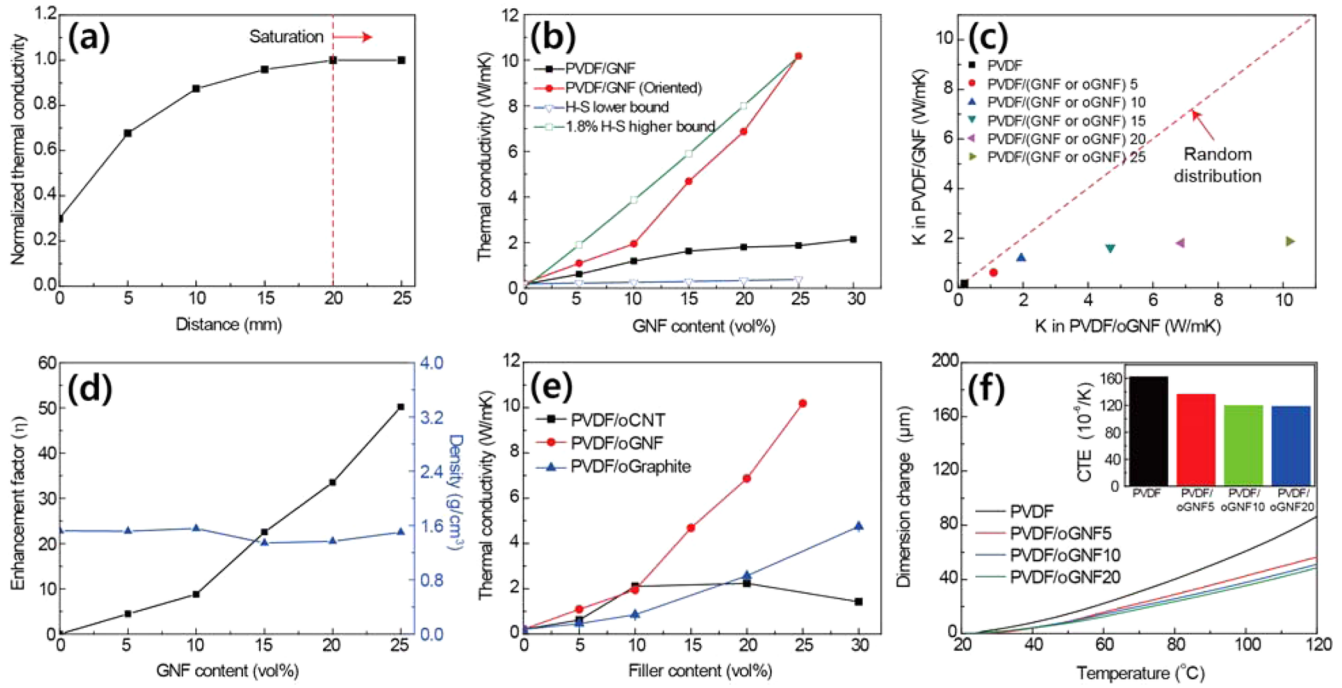

Figure 2. (a) Normalized *K* of PVDF/oGNF composites as a function of the L-shaped tube distance. A distance of zero corresponds to the kinked point of the tube. After the distance indicated by the dotted line, the *K* of a sample was saturated. (b) The variation of *K* values of PVDF/GNF and PVDF/oGNF composites with different GNF amount compared to the prediction from the Hashin−Shtrikman (H−S) model. (c) Ratios of *K* values for controlled PVDF/GNF to PVDF/oGNF composites as a function of GNF content. (d) Plots of TCE factors and densities of PVDF/oGNF composites as a function of GNF amount. (e) *K* values of PVDF composites containing MWCNTs, GNFs, and graphite as a function of filler content. (f) Dimensional change in neat PVDF and PVDF/oGNF composites with different GNF contents as a function of temperature. The inset shows the CTE values of the composites examined.

approximately 150 μm thick mat of PVDF and GNFs was developed in which GNFs were compressed with their surface normal preferentially aligned parallel to the normal film surface. A composite mat with preferentially oriented GNFs is expected to be beneficial for "in-plane" heat conduction through the numerous conductive pathways of GNFs, while "through-plane" heat conduction in which the majority of heat is transported along the surface normal of GNFs is limited because of a large surface−surface contact resistance between GNFs. To promote "through-plane" heat conduction of our composite, we employed an L-shaped kinked compression mold in such a way that GNFs were preferentially aligned in a PVDF/GNF composite film with their surfaces perpendicular to the film, as shown in the second step of Figure 1 and in Supporting Information Figure S1. The pieces of composite mat previously prepared were locked together with a cap and subsequently compressed under a pressure of 10 MPa at 180 °C for 5 min, which is above the melting temperature of PVDF (Supporting Information Figure S2). The pressure of 10 MPa was determined to optimize composite fabrication. During compression, the viscous mixture of molten PVDF and GNF passed through the parallel tube, thereby developing shear stress in the tube under a no slip assumption, leading to a cylindrical composite pillar, as shown in Figure 1. The composite pillar was carefully sliced into multiple circular disks, and samples approximately 0.2 cm thick were fabricated after surface polishing. It was expected that through-plane heat conduction would increase with GNF amount. For comparison, we also employed MWCNTs and graphite to investigate the geometric shape effect of carbon fillers on their orientation, as well as the resulting thermal conduction (Supporting Information Figure S3).

Our platform for oriented GNFs in a thermoplastic matrix with an L-shaped kinked tube offers a convenient way to examine the thermal conduction of the oGNFs depending upon tube position; the results are shown in Figure 2a. *K* was rapidly enhanced with increasing distance from the initial kinked position along the cylinder because of shear stress in the laminar flow of our molten composite at the tube surface arising from the variation of flow velocity from the tube surface to flow center was saturated after a distance of 2 cm. This implies that the orientation of GNFs was minimally improved beyond 2 cm in our process design. Since the *K* of a polymer composite is dominantly determined by thermally conductive fillers rather than the polymeric matrix with its intrinsically low *K* below 0.2 W/mK, control of the filler orientation is of prime importance with respect to heat conduction direction. Considering that most previous works were devoted to the development of filler orientation for high in-plane heat conduction,[28,29] our process offers an efficient way for fabricating an oriented composite suitable for applications such as TIM requiring high through-plane heat conduction with a relatively low filler amount.

The *K* values of PVDF/oGNF composites exponentially increased with GNF content and exhibited approximately 10.19 W/mK at 25 vol %, which was 50 times greater than the *K* value of a neat PVDF sample, as shown in Figure 2b. For comparison, the PVDF/GNF composites melt-compressed without using an L-shaped kinked tube were examined. The maximum *K* values of PVDF/GNF composites were approximately 2.14 W/mK with 30 vol % of GNFs, much lower than

DOI: 10.1021/acsami.5b02681
ACS Appl. Mater. Interfaces 2015, 7, 15256−15262

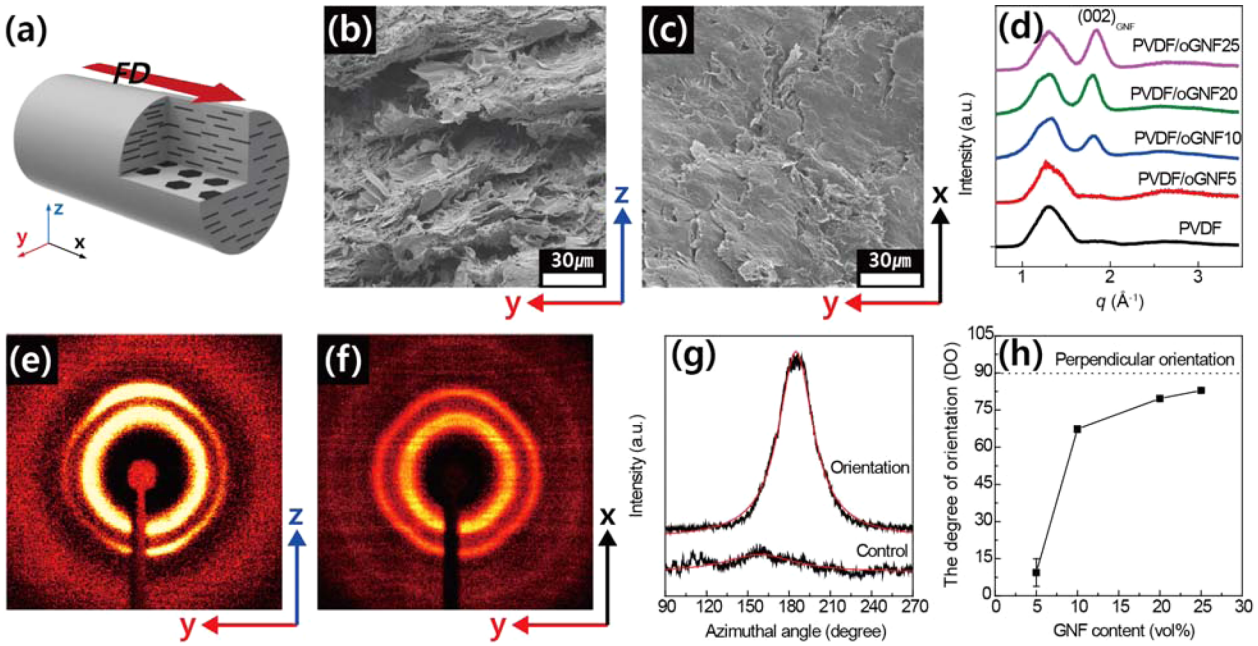

Figure 3. (a) Schematic illustration of PVDF/oGNF composite with GNFs preferentially aligned along the FD during the L-shaped kinked tube process. (b-c) SEM images of the fractured PVDF/oGNF composites in the *zy* and *xy* planes, respectively. (d) X-ray diffraction spectra of PVDF/oGNF composites as a function of GNF. (e, f) 2D X-ray scattering patterns of PVDF/oGNF composites in the *zy* and *xy* planes, respectively. (g) Azimuthal profile of the scattering pattern in (e). A profile of a scattering pattern from a controlled PVDF/GNF composite is also shown for comparison. (h) DO of PVDF/oGNF composites with GNF content. The values were calculated, based on Lorentzian distribution from the intensity distribution, as a function of azimuthal angle.

that with oGNFs from an L-shaped kinked tube. It should be noted that the maximum GNF loaded in PVDF was 25 vol % in our L-shape tube process above which a composite was very fragile without mechanical stability. Fabrication of a composite with GNF more than 25 vol % was not successful due to the lack of structural integrity of our composite. To prepare a disk-shape sample, polishing process on both surfaces should be done as noted in the experimental parts. A sample with the high GNF content was broken down during the polishing process, making it rarely possible to measure the thermal conduction properties of the sample. In our experimental conditions, a composite with 30 vol % unaligned GNFs was made with a proper mechanical stability. We do not, however, believe that the improved thermal conductivity due to the alignment of GNFs made the mechanical stability sacrificed. The electrical conduction behavior of the PVDF/oGNF composites is very similar to that of heat conduction, and the composites show very sharp increase in conduction with increasing GNF content. The overall behavior of the electrical conductivity is quite similar to that of other conduction filler containing polymer composites, indicative of typical percolative electric conduction (Supporting Information Figure S4).

We compared our results with oGNFs with a theoretical model based on effective medium prediction. The Hashin-Shtrikman (H−S) model, which is useful for high volume filler composites, was employed.[30,31] The H−S model represents two extreme lower and upper bounds of *K*. The lower bound considers the isolated medium in the continuum, and is calculated through a thermal resistance series model. The higher limit, on the other hand, considers a perfectly networked structure of the discrete medium in the continuum and is calculated through the conduction path by dispersed particles. The measured *K* of the composite with oriented GNFs coincides with the H−S lower bound values, but starts to exponentially increase beyond 5 vol % and reaches approximately 1.8% of the H−S higher bound at 25 vol % GNFs as shown in Figure 2b.

The enhancement of *K* by GNF orientation was further evaluated by examining the ratio of *K* values between controlled PVDF/GNF and PVDF/oGNF composites as a function of GNF content, as shown in Figure 2c. As expected, the neat PVDF samples prepared by melt-compression with and without the L-shaped kinked tube show very similar *K* values of approximately 0.17 and 0.19 W/mK, respectively and thus existed near the dotted line (ratio of *K* in PVDF/GNF to K in PVDF/oGNF = 1), which implies that shear stress present in the process rarely affects the polymer chain orientation, leading to samples with randomly entangled molecules. On the other hand, the values deviated from the dotted line when GNFs were present in the composites, which confirms that the orientation of GNFs through an L-shaped kinked tube was responsible for the enhanced *K*.

The high through-plane *K* of the PVDF/oGNF composite was further investigated using a thermal conductivity enhancement (TCE) factor, as shown in Figure 2d.[7] The value was determined by the enhanced *K* ratio of the matrix as $\eta = (K - K_m)/K_m$, where *k* is the thermal conductivity of the composites, and k_m is thermal conductivity of the matrix materials. Again, TCE increases with the amount of oGNFs in the composites, and a maximum of 50 was obtained in a PVDF/oGNF sample with 25 vol % GNFs. The results are notable considering that most composites with conventional fillers such as Al_2O_3, AlN, BN, and SiC show TCE values below 15 at 20 vol % due to the difficulty in controlling filler orientation in the polymer matrix.[28,29,32] Furthermore, our composites with oGNFs are lightweight with a density of approximately 1.5 g/cm^3 irrespective of the oGNF amount, as shown in Figure 2d.

DOI: 10.1021/acsami.5b02681
ACS Appl. Mater. Interfaces 2015, 7, 15256−15262

To further demonstrate the effectiveness of the oGNFs melt-compressed with an L-shaped kinked tube, we also incorporated one-dimensional MWCNT and three-dimensional graphite fillers into the PVDF matrix. The K values of both composites similarly increased with filler amount, as shown in Figure 2e and Supporting Information Figure S5a-b. However, the enhancement by the oriented fillers was significantly lower than that obtained by GNFs due to their low orientation during compression as shown later, which is consistent with the results previously reported with MWCNTs and graphite.[33] In the case of MWCNTs, the K value slightly decreased at high filler content possibly because of the entanglement between long nanotubes, making it difficult to align them along the FD.

Dimensional stability of a composite with temperature, characterized by the coefficient of thermal expansion (CTE), is very important for reliable thermal operation. Beneficially, the CTE of our composites along the x-direction, that is, FD decreases with oGNFs compared to that of neat PVDF = 162.09 ppm/°C, PVDF/oGNF5 = 136.35 ppm/°C, PVDF/oGNF10 = 119.45 ppm/°C to PVDF/oGNF20 = 118.26 ppm/°C, as shown in Figure 2f. The dimensional stability with oGNFs in our composites is ascribed to the negative CTE of GNFs in the planar direction.[34,35] As shown in Figure 2f, GNFs dominantly aligned with their surfaces perpendicular to the heat conduction direction efficiently compensate for thermal expansion of the PVDF matrix with temperature, leading to a composite with not only high thermal conduction, but also low CTE.

The proposed orientation of GNFs in our composites melt-compressed using an L-shaped kinked tube was confirmed by morphological analysis of the composites with microscopic and scattering tools, as shown in Figure 3. SEM results in the zy and xy planes of the oriented composite shown in Figure 3b and 3c, respectively, clearly show the preferred orientation of GNFs, corresponding to the scheme in which the surface normal of GNFs is aligned perpendicular to the FD, as illustrated in Figure 3a. The stacked edges of GNFs are dominantly visible in Figure 3b, while the flat and smooth surfaces of assembled GNFs are shown in Figure 3c. As expected, a controlled PVDF/GNF composite melt-compressed without an L-shape kinked tube exhibits randomly ordered GNFs, with some GNFs partially stacked along the compression direction (Supporting Information Figure S6a−c).

The preferred orientation of GNFs in our composite was also evidenced by X-ray scattering results. First, the powder diffraction results of the composites with different GNF contents in Figure 3d show that the diffraction peak appearing at 1.324 $Å^{-1}$ corresponding to the (200) reflection of PVDF crystals does not vary, whereas the peak at 1.861 $Å^{-1}$ corresponding to the (002) reflection of GNFs increases with GNFs content. To further reveal the preferred orientation, 2D X-ray scattering with different incident beam directions was performed as shown in Figure 3e and f and Supporting Information Figure S7. With the incident beam along the x-axis (zy plane), the (002) reflection was intensified at meridian regions (the northern regions of the diffraction patterns), as shown in Figure 3e, which confirms the orientation of GNFs visualized in Figure 3b. Ring shape (002) scattering of GNFs was observed with the incident beam along the z-axis (xy plane), as shown in Figure 3f; the results are again consistent with the real space morphology shown in Figure 3c. It should be also noted that the 2D X-ray scattering results show ring shape reflections near q of 1.324 $Å^{-1}$ corresponding to the (200) reflection of PVDF crystals, indicative of randomly ordered PVDF crystals. Azimuthal plots of (002) reflections of an oriented composite and a control composite, both with 25 vol % of GNFs, as in Figure 3g, clearly show the preferred orientation of GNFs processed in the L-shaped kinked tube.[36,37] As expected, 2D X-ray scattering results show that orientation of GNFs was rarely observed in the controlled PVDF/GNF composite. In addition, composites with CNT as well as graphite processed in L-shape tube exhibited very low orientation in 2D X-ray scattering pattern, consistent with K results in Figure 2e.

The scattering intensity $I(\Phi)$ from the azimuthal scan was fitted by a Lorentzian function. The degree of orientation (DO) for GNFs in a composite was determined from the intensity distribution of the (002) reflection of the Debye ring using the following equation: $DO = ((360° - \Delta\Phi)/360°) \times 100$, where $\Delta\Phi$ is the full-width of degree at half-maximum of the diffraction peak in the in-plane XRD profile.[38] Most of the PVDF/oGNF composites exhibited high GNF DO greater than 65, and the DO values slightly increased with filler content. The low DO in the 5 vol % composite may be due to the weak flake-to-flake interaction at such a low filler content. When the content increased, GNFs efficiently interacted with each other and collectively aligned during the process, leading to high DO values.[39] To elucidate the effect of crystalline polymer structure of PVDF on orientation of GNFs, we prepared amorphous polystyrene (PS)/oriented GNF composites with the same procedure. The composite also exhibited (002) reflection intensified due to oriented GNF at meridian regions against the incident beam along the x-axis (Supporting Information Figure S8). The resulting azimuthal plots of (002) reflection of the PS/oriented GNF composite exhibited high DO value of approximately 77, similar to the results with PVDF. Consequently, the orientation of GNF fillers were dominantly affected by shear force in L-shaped kinked tube. Therefore, our approach can serve a platform to prepare polymer composites with highly aligned GNF fillers regardless of the type of polymers.

The temperature-dependent K variation in our oriented composite was examined, and the results are shown in Figure 4a. No significant change in K was observed with a PVDF/oGNF 25 vol % up to 150 °C due to the high melting temperature (~165 °C) of PVDF (Supporting Information Figure S2). In addition, the derived temperature durability test included multiple heating and cooling cycles between room temperature and 150 °C; again, a very reliable K value was observed even after 20 cycles, as shown in Figure 4b. It should be noted that most polymer filled composites exhibit a decrease in thermal diffusivity because of the increased phonon scattering with temperature, while specific heat decreases with temperature. K in general decreases when a composite is heated because of the decrease of the composite density arising from expansion of the polymer matrix. In our GNF oriented composites, the similar behavior was observed in thermal diffusivity and specific heat with temperature (Supporting Information Figure S9). We speculate that the small variation of K with temperature is attributed to the negative coefficient of thermal expansion of GNFs in the planar direction (Figure 2f). Such a small variation of K with temperature would be beneficial for long-term device operation.

To further demonstrate the heat sink performance of our PVDF/oGNF composites for practical operation, we visualized the heat accumulation and release properties of a PVDF/oGNF

DOI: 10.1021/acsami.5b02681
ACS Appl. Mater. Interfaces 2015, 7, 15256−15262

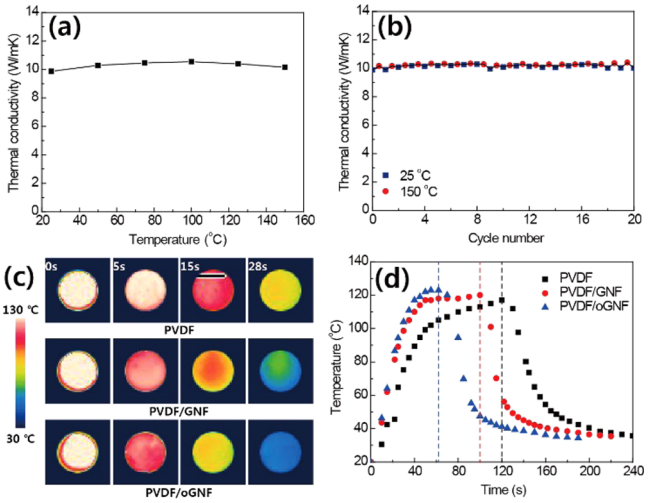

Figure 4. K variation of a PVDF/oGNF composite with 25 vol % of GNF (a) with temperature and (b) upon multiple heating and cooling cycles. (c) Infrared images of neat PVDF, PVDF/GNF, and PVDF/oGNF composites upon cooling. The temperature gradient scale bar at left shows the highest and lowest temperatures of 130 and 30 °C, respectively. (d) Surface temperature variation of the neat PVDF, PVDF/GNF, and PVDF/oGNF composites with time upon heating and cooling events. Cooling started at the dotted line for each sample.

composite with 25 vol % GNFs mounted on a heat source with an infrared camera as shown in Figure 4c. While the neat PVDF sample was slowly cooled to room temperature from approximately 130 °C, the sample with randomly ordered GNFs exhibited faster cooling behaviors, as shown in the second row of Figure 4c. The composite containing oGNFs rapidly cooled to approximately 45 °C within 28 s. Quantitative heating and cooling results based on infrared imaging, as shown in Figure 4d, clearly illustrate high heat release performance.

CONCLUSIONS

We demonstrated a simple but robust process to control GNF orientation in a polymer matrix for high-performance through-plane heat conduction. Our method is based on melt-compression of a composite through an L-shaped kinked tube. The preferred orientation of GNFs in the composites was achieved during the process in which the surfaces of GNFs were aligned perpendicular to the FD of molten polymer. The oriented GNFs allowed for facile formation of numerous conduction pathways along the FD, giving rise to a high through-plane thermal conductivity greater than 10 W/mK in the composite containing 25 vol % GNFs. Our thermally conductive composite with its density of approximately 1.5 g/cm^3 was dimensionally stable with a low coefficient of thermal expansion, and its high thermal conductivity was successfully maintained up to 150 °C, even after multiple heating and cooling cycles. The performance of our oriented composite during rapid heating and cooling was characterized by infrared image analysis and suggests that our approach is an efficient way to fabricate high through-plane thermal interface materials for various microelectronic packaging applications.

ASSOCIATED CONTENT

Supporting Information

Photographs of the L-shaped kinked tube (Figure S1), DSC trace of neat PVDF (Figure S2), SEM images of fillers (Figure S3), electrical conductivity of PVDF/oGNF composites (Figure S4), thermal conductivities of PVDF/MWCNT, PVDF/oriented MWCNT, PVDF/graphite, and PVDF/oriented graphite composites (Figure S5), SEM images of PVDF/GNF composite (Figure S6), 2D X-ray scattering patterns of PVDF/oGNF, PVDF/oriented MWCNT and PVDF/oriented graphite composites (Figure S7), 2D X-ray scattering pattern and azimuthal profile of PS/oGNF composite (Figure S8), temperature-dependent thermal diffusivity and specific heat of PVDF/oGNF composite (Figure S9), and thermal conductivities of various composites (Table S1). The Supporting Information is available free of charge on the ACS Publications website at DOI: 10.1021/acsami.5b02681.

AUTHOR INFORMATION

Corresponding Authors

*E-mail: koo@kist.re.kr. Phone: +82-02-958-6872.
*E-mail: cmpark@yonsei.ac.kr. Phone: +82-2-2123-2833. Fax: +82-2-312-5375.

Author Contributions

‖H.J. and S.Y. contributed equally.

Notes

The authors declare no competing financial interest.

ACKNOWLEDGMENTS

This project was supported by DAPA, ADD and a grant from the National Research Foundation of Korea (NRF), funded by the Korean government (MEST) (No. 2014R1A2A1A01005046).

ABBREVIATIONS

PVDF = poly(vinylidene fluoride)
GNF = graphene nanoflake
K = thermal conductivity
TIM = thermal interface material
TBR = thermal boundary resistances
FD = flow direction
DMF = *N*,*N*′-dimethylformamide
MWCNT = multiwalled carbon nanotubes
TMA = thermomechanical analysis
TCE = thermal conductivity enhancement
CTE = coefficient of thermal expansion
PS = polystyrene

REFERENCES

(1) Yan, Z.; Liu, G.; Khan, J. M.; Balandin, A. A. Graphene Quilts for Thermal Management of High-Power Gan Transistors. *Nat. Commun.* **2012**, *3*, 827.
(2) Koo, B.; Goli, P.; Sumant, A. V.; dos Santos Claro, P. C.; Rajh, T.; Johnson, C. S.; Balandin, A. A.; Shevchenko, E. V. Toward Lithium Ion Batteries with Enhanced Thermal Conductivity. *ACS Nano* **2014**, *8*, 7202−7207.
(3) Schleeh, J.; Mateos, J.; Iniguez-de-la-Torre, I.; Wadefalk, N.; Nilsson, P. A.; Grahn, J.; Minnich, A. J. Phonon Black-Body Radiation Limit for Heat Dissipation in Electronics. *Nat. Mater.* **2015**, *14*, 187−192.
(4) Han, N.; Viet Cuong, T.; Han, M.; Deul Ryu, B.; Chandramohan, S.; Bae Park, J.; Hye Kang, J.; Park, Y.-J.; Bok Ko, K.; Yun Kim, H.; Kyu Kim, H.; Hyoung Ryu, J.; Katharria, Y. S.; Choi, C.-J.; Hong, C.-H. Improved Heat Dissipation in Gallium Nitride Light-Emitting Diodes with Embedded Graphene Oxide Pattern. *Nat. Commun.* **2013**, *4*, 1452.
(5) Ji, H.; Sellan, D. P.; Pettes, M. T.; Kong, X.; Ji, J.; Shi, L.; Ruoff, R. S. Enhanced Thermal Conductivity of Phase Change Materials with

DOI: 10.1021/acsami.5b02681
ACS Appl. Mater. Interfaces 2015, 7, 15256−15262

Ultrathin-Graphite Foams for Thermal Energy Storage. *Energy Environ. Sci.* **2014**, *7*, 1185−1192.
(6) Goyal, V.; Sumant, A. V.; Teweldebrhan, D.; Balandin, A. A. Direct Low-Temperature Integration of Nanocrystalline Diamond with Gan Substrates for Improved Thermal Management of High-Power Electronics. *Adv. Funct. Mater.* **2012**, *22*, 1525−1530.
(7) Shahil, K. M. F.; Balandin, A. A. Graphene−Multilayer Graphene Nanocomposites as Highly Efficient Thermal Interface Materials. *Nano Lett.* **2012**, *12*, 861−867.
(8) Wang, S.; Cheng, Y.; Wang, R.; Sun, J.; Gao, L. Highly Thermal Conductive Copper Nanowire Composites with Ultralow Loading: Toward Applications as Thermal Interface Materials. *ACS Appl. Mater. Interfaces* **2014**, *6*, 6481−6486.
(9) Yu, S.; Lee, J.-W.; Han, T. H.; Park, C.; Kwon, Y.; Hong, S. M.; Koo, C. M. Copper Shell Networks in Polymer Composites for Efficient Thermal Conduction. *ACS Appl. Mater. Interfaces* **2013**, *5*, 11618−11622.
(10) Tanimoto, M.; Yamagata, T.; Miyata, K.; Ando, S. Anisotropic Thermal Diffusivity of Hexagonal Boron Nitride-Filled Polyimide Films: Effects of Filler Particle Size, Aggregation, Orientation, and Polymer Chain Rigidity. *ACS Appl. Mater. Interfaces* **2013**, *5*, 4374−4382.
(11) Yoshihara, S.; Ezaki, T.; Nakamura, M.; Watanabe, J.; Matsumoto, K. Enhanced Thermal Conductivity of Thermoplastics by Lamellar Crystal Alignment of Polymer Matrices. *Macromol. Chem. Phys.* **2012**, *213*, 2213−2219.
(12) Mamunya, Y. P.; Davydenko, V. V.; Pissis, P.; Lebedev, E. V. Electrical and Thermal Conductivity of Polymers Filled with Metal Powders. *Eur. Polym. J.* **2002**, *38*, 1887−1897.
(13) Bonnet, P.; Sireude, D.; Garnier, B.; Chauvet, O. Thermal Properties and Percolation in Carbon Nanotube-Polymer Composites. *Appl. Phys. Lett.* **2007**, *91*, 201910.
(14) Tian, X.; Itkis, M. E.; Bekyarova, E. B.; Haddon, R. C. Anisotropic Thermal and Electrical Properties of Thin Thermal Interface Layers of Graphite Nanoplatelet-Based Composites. *Sci. Rep.* **2013**, *3*, 1710.
(15) Yu, A.; Ramesh, P.; Sun, X.; Bekyarova, E.; Itkis, M. E.; Haddon, R. C. Enhanced Thermal Conductivity in a Hybrid Graphite Nanoplatelet − Carbon Nanotube Filler for Epoxy Composites. *Adv. Mater.* **2008**, *20*, 4740−4744.
(16) Taphouse, J. H.; Smith, O. N. L.; Marder, S. R.; Cola, B. A. A Pyrenylpropyl Phosphonic Acid Surface Modifier for Mitigating the Thermal Resistance of Carbon Nanotube Contacts. *Adv. Funct. Mater.* **2014**, *24*, 465−471.
(17) Clancy, T. C.; Gates, T. S. Modeling of Interfacial Modification Effects on Thermal Conductivity of Carbon Nanotube Composites. *Polymer* **2006**, *47*, 5990−5996.
(18) Lin, Z.; Liu, Y.; Raghavan, S.; Moon, K.-s.; Sitaraman, S. K.; Wong, C.-p. Magnetic Alignment of Hexagonal Boron Nitride Platelets in Polymer Matrix: Toward High Performance Anisotropic Polymer Composites for Electronic Encapsulation. *ACS Appl. Mater. Interfaces* **2013**, *5*, 7633−7640.
(19) Cho, H.-B.; Tokoi, Y.; Tanaka, S.; Suematsu, H.; Suzuki, T.; Jiang, W.; Niihara, K.; Nakayama, T. Modification of Bn Nanosheets and Their Thermal Conducting Properties in Nanocomposite Film with Polysiloxane According to the Orientation of Bn. *Compos. Sci. Technol.* **2011**, *71*, 1046−1052.
(20) Lim, H. S.; Oh, J. W.; Kim, S. Y.; Yoo, M.-J.; Park, S.-D.; Lee, W. S. Anisotropically Alignable Magnetic Boron Nitride Platelets Decorated with Iron Oxide Nanoparticles. *Chem. Mater.* **2013**, *25*, 3315−3319.
(21) Cho, H.-B.; Konno, A.; Fujihara, T.; Suzuki, T.; Tanaka, S.; Jiang, W.; Suematsu, H.; Niihara, K.; Nakayama, T. Self-Assemblies of Linearly Aligned Diamond Fillers in Polysiloxane/Diamond Composite Films with Enhanced Thermal Conductivity. *Compos. Sci. Technol.* **2011**, *72*, 112−118.
(22) Marconnet, A. M.; Yamamoto, N.; Panzer, M. A.; Wardle, B. L.; Goodson, K. E. Thermal Conduction in Aligned Carbon Nanotube−Polymer Nanocomposites with High Packing Density. *ACS Nano* **2011**, *5*, 4818−4825.
(23) Yorifuji, D.; Ando, S. Enhanced Thermal Conductivity over Percolation Threshold in Polyimide Blend Films Containing Zno Nano-Pyramidal Particles: Advantage of Vertical Double Percolation Structure. *J. Mater. Chem.* **2011**, *21*, 4402−4407.
(24) Lovinger, A. Poly(Vinylidene Fluoride). In *Developments in Crystalline Polymers—1*; Bassett, D. C., Ed.; Springer: Netherlands, 1982; Chapter 5, pp 195−273.
(25) Levi, N.; Czerw, R.; Xing, S.; Iyer, P.; Carroll, D. L. Properties of Polyvinylidene Difluoride−Carbon Nanotube Blends. *Nano Lett.* **2004**, *4*, 1267−1271.
(26) Ansari, S.; Giannelis, E. P. Functionalized Graphene Sheet—Poly(Vinylidene Fluoride) Conductive Nanocomposites. *J. Polym. Sci., Part B: Polym. Phys.* **2009**, *47*, 888−897.
(27) Yu, J.; Huang, X.; Wu, C.; Jiang, P. Permittivity, Thermal Conductivity and Thermal Stability of Poly(Vinylidene Fluoride)/Graphene Nanocomposites. *IEEE Trans. Dielectr. Electr. Insul.* **2011**, *18*, 478−484.
(28) Yu, S.; Kim, D.-K.; Park, C.; Hong, S.; Koo, C. Thermal Conductivity Behavior of Sic−Nylon 6,6 and Hbn−Nylon 6,6 Composites. *Res. Chem. Intermed.* **2014**, *40*, 33−40.
(29) Ohashi, M.; Kawakami, S.; Yokogawa, Y.; Lai, G.-C. Spherical Aluminum Nitride Fillers for Heat-Conducting Plastic Packages. *J. Am. Ceram. Soc.* **2005**, *88*, 2615−2618.
(30) Hashin, Z.; Shtrikman, S. A Variational Approach to the Theory of the Effective Magnetic Permeability of Multiphase Materials. *J. Appl. Phys.* **1962**, *33*, 3125−3131.
(31) Choi, J. R.; Yu, S.; Jung, H.; Hwang, S. K.; Kim, R. H.; Song, G.; Cho, S. H.; Bae, I.; Hong, S. M.; Koo, C. M.; Park, C. Self-Assembled Block Copolymer Micelles with Silver-Carbon Nanotube Hybrid Fillers for High Performance Thermal Conduction. *Nanoscale* **2015**, *7*, 1888−1895.
(32) Balandin, A. A. Thermal Properties of Graphene and Nanostructured Carbon Materials. *Nat. Mater.* **2011**, *10*, 569−581.
(33) Shahil, K. M. F.; Balandin, A. A. Thermal Properties of Graphene and Multilayer Graphene: Applications in Thermal Interface Materials. *Solid State Commun.* **2012**, *152*, 1331−1340.
(34) Nelson, J. B.; Riley, D. P. The Thermal Expansion of Graphite from 15°C. To 800°C.: Part I. Experimental. *Proc. Phys. Soc.* **1945**, *57*, 477−486.
(35) Yoon, D.; Son, Y.-W.; Cheong, H. Negative Thermal Expansion Coefficient of Graphene Measured by Raman Spectroscopy. *Nano Lett.* **2011**, *11*, 3227−3231.
(36) Forsyth, P. A., Jr; Marčelia, S.; Mitchell, D. J.; Ninham, B. W. Ordering in Colloidal Systems. *Adv. Colloid Interface Sci.* **1978**, *9*, 37−60.
(37) Davis, V. A.; Ericson, L. M.; Parra-Vasquez, A. N. G.; Fan, H.; Wang, Y.; Prieto, V.; Longoria, J. A.; Ramesh, S.; Saini, R. K.; Kittrell, C.; Billups, W. E.; Adams, W. W.; Hauge, R. H.; Smalley, R. E.; Pasquali, M. Phase Behavior and Rheology of Swnts in Superacids. *Macromolecules* **2004**, *37*, 154−160.
(38) Fukumoto, H.; Nagano, S.; Kawatsuki, N.; Seki, T. Photo-Alignment Behavior of Mesoporous Silica Thin Films Synthesized on a Photo-Cross-Linkable Polymer Film. *Chem. Mater.* **2006**, *18*, 1226−1234.
(39) Kim, H.; Macosko, C. W. Processing-Property Relationships of Polycarbonate/Graphene Composites. *Polymer* **2009**, *50*, 3797−3809.

DOI: 10.1021/acsami.5b02681
ACS Appl. Mater. Interfaces 2015, 7, 15256−15262